IEEE Photonics Journal
An IEEE Photonics Society Publication

Characterization of Mid-Infrared Silicon-on-Sapphire Microring Resonators With Thermal Tuning

Volume 4, Number 4, August 2012

Chi Yan Wong, Student Member, IEEE
Zhenzhou Cheng, Student Member, IEEE
Xia Chen, Member, IEEE
Ke Xu, Student Member, IEEE
Christy K. Y. Fung, Student Member, IEEE
Yi Min Chen, Student Member, IEEE
Hon Ki Tsang, Senior Member, IEEE

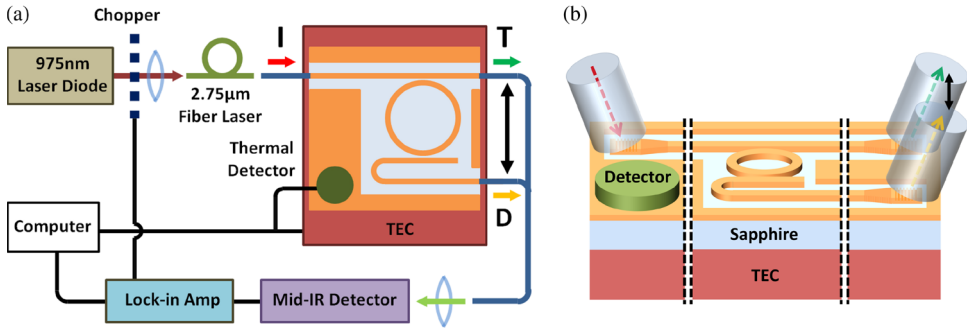

DOI: 10.1109/JPHOT.2012.2204734
1943-0655/$31.00 ©2012 IEEE

Characterization of Mid-Infrared Silicon-on-Sapphire Microring Resonators With Thermal Tuning

Chi Yan Wong, *Student Member, IEEE*, Zhenzhou Cheng, *Student Member, IEEE*, Xia Chen, *Member, IEEE*, Ke Xu, *Student Member, IEEE*, Christy K. Y. Fung, *Student Member, IEEE*, Yi Min Chen, *Student Member, IEEE*, and Hon Ki Tsang, *Senior Member, IEEE*

Department of Electronic Engineering, The Chinese University of Hong Kong, Shatin, Hong Kong

DOI: 10.1109/JPHOT.2012.2204734

Manuscript received May 4, 2012; revised June 5, 2012; accepted June 7, 2012. Date of publication June 13, 2012; date of current version June 28, 2012. This work was supported by Hong Kong UGC Special Equipment Grant CUHK-SEG01 Grant and direct Grant 2050508. Corresponding author: C. Y. Wong (e-mail: cywong@ee.cuhk.edu.hk).

Abstract: Microring resonators on silicon-on-sapphire (SOS) were characterized at 2.75 μm wavelength. We obtained a Q factor of 11400 $\pm$ 800. The thermo-optic coefficient of epitaxial silicon of SOS wafer was measured to be $2.11 \pm 0.08 \times 10^{-4}$ K^{-1}. We also describe a characterization technique to measure the Q of microring resonators using a fixed wavelength source. By only varying the temperature of the device, it is possible to measure the Q of a mid-infrared (mid-IR) microresonator. The proposed method provides an alternative method of Q measurement for microring resonators in mid-IR, where tunable lasers may not be easily available. The technique was used to determine the Q of SOS microring resonators at 2.75 μm wavelength.

Index Terms: Integrated nanophotonic systems, mid-infrared (mid-IR), silicon nanophotonics, silicon-on-sapphire (SOS), temperature, waveguide devices.

1. Introduction

Silicon photonics in mid-infrared (mid-IR), of 2–6 μm, have attracted a great interest because of their potential applications in chemical sensing, infrared spectroscopy and free-space communications [1], [2]. Moreover, due to the absence of two-photon absorption (TPA) in mid-IR range, the applications of optical nonlinearities in silicon can be faster and more efficient because of the absence of free-carriers generated by TPA [3]–[7]. Unfortunately, the conventional silicon-on-insulator (SOI) based devices are not suitable for mid-IR, because the buried oxide (BOX) layer has high absorption at wavelengths between 2.6–6.0 μm (with a narrow transparent window around 3.2 μm) [1], [8], [9]. Nevertheless, silicon-on-sapphire (SOS) provides an alternative potential platform for mid-IR devices due to the high transparency of sapphire in mid-IR [1]. SOS based waveguides have been proposed and demonstrated experimentally in the wavelength range of 1.5–5.6 μm [10], [11]. Recently, microring resonators were reported operating in the 5.5 μm wavelength range [12].

In the 2.6–3.0 μm range, there are a number of potential applications of microresonators for chemical sensing and nonlinear generation of mid-IR light. The vibrational and rotational resonances of most gas molecules fall within the mid-IR spectral range: for example the hydroxyl (OH) group have strong absorption peaks spectrum around 2.7 μm [13], and thus the sensitivity of

evanescent optical waveguide based sensors [14], [15], may be sufficient to detect trace concentrations. Nonlinearities in the mid-IR are also of interest for use in generating different mid-IR wavelengths such as mid-IR silicon Raman amplifier/laser [4], [5], or optical parametric amplifiers [6], [7]. High-Q microresonators can build up high electric energy density in the cavity, which can thus enhance the effective nonlinearity of microresonators. At telecom wavelengths, TPA in silicon and the long lived free-carriers produced by TPA will lead to shifts in resonances which limit the possible enhancement of optical nonlinearities in silicon microresonators. As mentioned previously, TPA is absent in silicon at mid-IR wavelengths and thus the measurement of Q in microresonators at mid-IR wavelengths is of interest for possible applications in nonlinear mid-IR devices. However, the measurement method of Q at mid-IR is limited. In the 2.6–3.0 μm range, there is a lack of narrow linewidth tunable laser sources. In the 3–6 μm range, the conventional quantum cascade lasers (QCLs) provide limited spectral resolution in the order of 0.1 nm and set a limit on the maximum measurable Q using this source. In order to overcome the limitation of the laser source, there is a need of an alternative Q measurement method with narrow linewidth laser sources such as a mid-IR He-Ne laser.

For high-Q resonator based devices, thermal stability is crucial in practical usage. The thermo-optic coefficient of silicon is higher than silica, and has a value of $(1.86 \pm 0.08) \times 10^{-4}$ K^{-1} at 1.5 μm wavelength [16]. Silicon waveguide devices are thus more sensitive to temperature than devices based on silica [17]. The thermo-optic coefficient of bulk silicon has been measured in mid-IR range up to 6.0 μm [18]. However, the value of strained silicon thin film such as epitaxial layer of SOS have not been studied in mid-IR range as it is difficult to form a conventional etalon (such as described in [16]) since the thickness of the silicon layer can be less than the wavelength in the mid-IR range.

In this paper, we report on the measurement of the thermo-optic coefficient of SOS waveguides and Q factor measurement of microresonators at a wavelength of 2.75 μm. We fabricated mid-IR microring resonators which support a fundamental quasi-transverse electric (quasi-TE) mode. The devices were characterized by thermal tuning using a fixed wavelength Er/Pr-codoped ZrF_4-BaF_2-LaF_3-AlF_3-NaF (ZBLAN) fiber laser at 2.75 μm [19]. A method of Q factor estimation from temperature scanning transmission curve is proposed, which is different from the method used in our previous work [20] as it does not need any curve fitting. Similar results are obtained if we assume the ratio of resonant period (in temperature) to the full-width-half-maximum (FWHM) of resonant dip/peak, $\Delta T/\delta T$, is equal to the cavity finesse [21]. Finally, the thermo-optic coefficient of the epitaxial silicon layer of SOS is also estimated by perturbation method [22], [23]. The measurement techniques were verified with conventional SOI microring resonators in near-infrared (near-IR).

2. Design and Fabrication

The silicon strip waveguides were fabricated on SOS with 600 nm thickness and 950 nm width which satisfy the single mode condition of quasi-TE mode at 2.75 μm. The corresponding electric field mode profile are calculated by finite element method (FEM), shown as Fig. 1(c), with refractive indices of 3.44 (silicon), 1.72 (sapphire) and 1 (air) in mid-IR at room temperature [24]. For microring resonators, in order to have a better control of the coupling between the ring cavities and the bus waveguides, the race-track type geometry was used. They were fabricated with 45 μm coupling length and 150 μm bending radius and, thus, with 1032 μm round-trip length. According to simulations using beam propagation method, the bending loss of the waveguides with 150 μm bending radius is theoretically negligible compared to the propagation loss of the waveguides. In this paper, microring resonators with two bus waveguides were used. In order to simply the design, the two bus waveguides of each resonator have identical coupling lengths and separation from the ring waveguide.

Grating couplers are used for coupling mid-IR light between the SOS waveguides and single mode ZBLAN fibers with a 10° off-vertical orientation [25], as shown in Fig. 2(b). The uniform-1-D gratings were 360 nm shallow-etched in a period of 1.055 μm and 0.31 fill factor. They also ensure

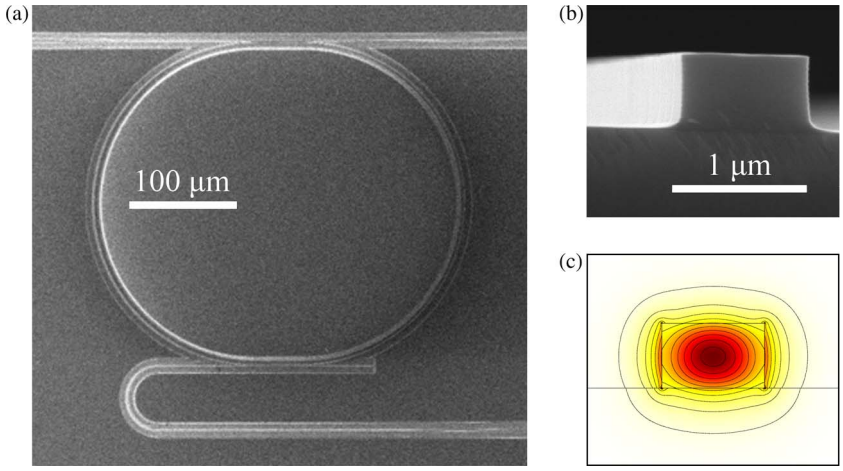

Fig. 1. (a) SEM image of the race-track microring resonator with 150 μm bending radius and 1032 μm round-trip length. (b) SEM image of waveguide cross section. (c) Electrical field mode profile of corresponding quasi-TE mode, calculated by FEM.

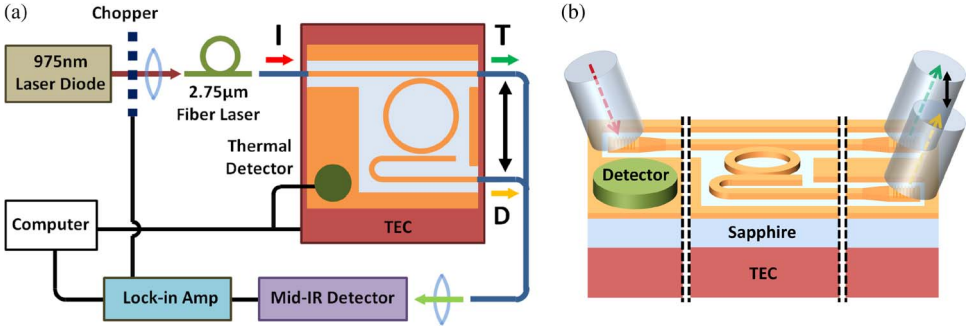

Fig. 2. Schematic diagram of measurement setup, (a) Mid-IR light coupled into input port $(\mathbf{I})$ and coupled out from throughput port $(\mathbf{T})$ or drop port $(\mathbf{D})$ of the microring resonator on SOS. The temperature of the silicon waveguide is controlled by the TEC attached under the sample and acquired by thermal detector direct attached on the epitaxial silicon. The output signal is collected by mid-IR photodiode with lock-in amplifier and mechanical chopped pump laser. (b) The input light coupled in (red) from undoped ZBLAN fiber to the input port of the microring resonator and coupled out to the fiber from either throughput port (green) or drop port (yellow) through grating couplers.

the light polarization of waveguides and rings in quasi-TE mode. The microring resonators and grating couplers were patterned by electron beam lithography with ZEP520A resist and then dry etched by reactive-ion etching with C_4F_8 and SF_6 mixture. The scanning electron microscope (SEM) images of the fabricated microring resonator and the strip waveguide cross-section are shown in Fig. 1(a) and (b).

For comparison in near-IR, a SOI microring resonator (quasi-TE mode) was fabricated on a wafer with 220 nm top silicon layer and 2 μm BOX by deep-UV lithography. The waveguide width and round-trip length are 500 nm and 264 μm, respectively.

3. Experimental Setup

The experimental setup is shown in Fig. 2. The Er/Pr-codoped ZBLAN fiber laser with lasing wavelength at 2.75 μm and linewidth $<$ 0.12 nm was pumped by a high power 975 nm diode laser. The mid-IR light from the laser was coupled to an undoped ZBLAN fiber. And then the light is coupled from undoped ZBLAN fiber to the input of the resonator through grating coupler. Another fiber collected the output light from either the throughput port or the drop port of the resonator by

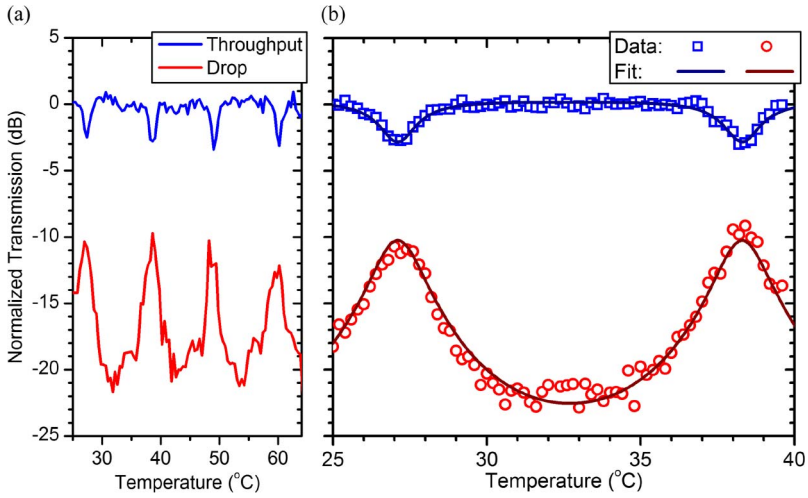

Fig. 3. Normalized temperature dependence transmission of the quasi-TE microring with 1032 μm round-trip length. (a) Temperature scanning at 25–65 °C of throughput port (blue) and drop port (red). (b) Temperature scanning at 25–40 °C of throughput port (blue squares) and drop port (red circles) with theoretical fitting curves.

grating couplers. Finally, the output light was captured by a mid-IR photovoltaic detector. In order to increase the signal-to-noise ratio, the signal of the mid-IR detector was measured by a lock-in amplifier with a mechanical chopper modulating the pump laser. The SOS chip was mounted on top of a thermoelectric cooler (TEC) for temperature tuning. A thermal detector was directly attached on the epitaxial silicon for monitoring the temperature and TEC control feedback. The light from the throughput port and drop port was measured at 25–65 °C. The received signal is finally normalized by the output of a reference straight waveguide in order to remove the temperature dependence of the coupling efficiency of the grating couplers. In the case of SOI microring measurement, the fibers, laser source, and detector were replaced by fused silica single-mode fibers, a tunable laser, and an optical power meter for near-IR.

4. Results and Analysis

4.1. Temperature Dependent Transmission

The temperature dependent transmission of the highest Q ring, with 350 nm separation between bus waveguides and ring, is plotted in Fig. 3. By tuning the temperature between 25–65 °C, we can observe four resonances in both throughput and drop ports with ~11 °C temperature spacing and extinction ratio of ~10 dB from the drop port. There is ~10 dB loss from the drop port at resonance compared to the reference waveguide (without resonator). The fluctuations of the measurement data in Fig. 3(a) may be due to instability in the fiber laser as there laser longitudinal mode hopping and wavelength drift noise may be present during temperature scanning of the microresonator. The measured results could be improved by reducing the temperature scan range (25–40 °C), as shown in Fig. 3(b).

The measured transmittance was analyzed by a theoretical model of the microresonator [26]:

$$\frac{E_t}{E_i} = \frac{t(e^{-i\theta} - \alpha)}{e^{-i\theta} - \alpha t^2}, \quad \frac{E_d}{E_i} = \frac{i\sqrt{\alpha}\kappa^2 e^{i\theta'}}{1 - \alpha t^2 e^{i\theta}}, \quad \theta = \frac{2\pi L_{rt} n_{eff}}{\lambda_o} \tag{1}$$

with temperature, T, dependent round-trip phase shift $\theta(T) = \theta(T_o) + \Delta\theta(T)$:

$$\Delta\theta(T) \cong 2\pi L_{rt} \frac{\partial n_{eff}}{\partial T}\bigg|_{\lambda_o} \frac{T - T_o}{\lambda_o} \tag{2}$$

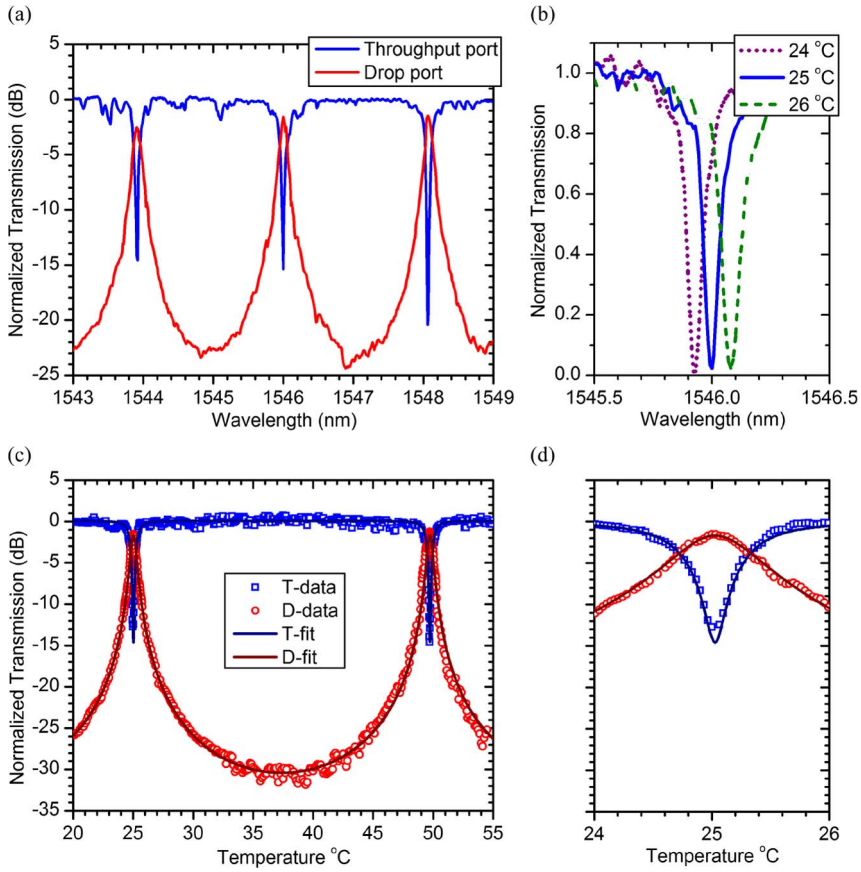

Fig. 4. Normalized transmission curves of quasi-TE microring with 264 μm round-trip length. (a) Wavelength scanning at 25 °C. (b) Temperature dependent resonant dip of throughput port in linear scale. (c)–(d) Temperature scanning at 20–55 °C and 24–26 °C fixed in 1546 nm with theoretical fitting curves.

where E_i, E_t, and E_d are the electric field at input port, throughput port, and drop port, respectively; α is the field round-trip loss factor; t and κ are the field coupling coefficients of each bus waveguides and ring with $|t|^2 + |\kappa|^2 = 1$ where $t = t_1 = t_2$ and $\kappa = \kappa_1 = \kappa_2$. The "1" and "2" subscripts refer to the each bus waveguides, respectively; θ' is the phase shift reached to the drop port with half of the round-trip; L_{rt} is the physical round-trip length; n_{eff} is the effective index of the waveguide mode; λ_o is the wavelength in vacuum; T_o is the reference temperature; $\partial n_{eff}/\partial T$ is the thermo-optic coefficient of the waveguide mode which depends on the waveguide material (air, silicon and sapphire) and the mode field profile. In order to simplify the model, the propagation loss and the coupling efficiency between the waveguides and the ring are assumed to be temperature independent. Moreover, the linear thermal expansion of silicon is in the order of 10^{-6} K^{-1} [27] which is two orders of magnitude less than the thermo-optic effect of silicon, and therefore neglected in our analysis. The fitting curves of temperature scanning of the microring, shown in Fig. 3(b), agree well with the experimental data with fitting parameters $\alpha = 0.71$, $|t| = 0.93$ and $n_{eff} = 2.72$. There are fluctuation in the measured values at the drop port, between normalized level -21 dB and -23 dB because of the noise background of the setup.

4.2. Quality Factor

In order to develop and verify the method for Q factor estimation from temperature dependent transmission curve, we can start with a conventional SOI microring for near-IR. The transmission spectrum at 25 °C is shown in Fig. 4(a), which shows the free-spectral-range (FSR) as

2.08 $\pm$ 0.014 nm. Fig. 4(b) shows the resonant dip of the throughput port centered at 1546 nm with FWHM $\delta\lambda_o = 0.08 \pm 0.014$ nm. The corresponding Q factor is about 19900 $\pm$ 3500. The figure also shows the resonant wavelength red (blue) shifted with increasing (decreasing) the temperature. We can see that the shape of the spectral profile of the resonant dip is almost unchanged in this temperature range. For the thermal tuning measurement, we fixed the laser wavelength at the resonant wavelength at 25 °C (1546 nm) and tuned the temperature. When the resonance is shifted by about half of $\delta\lambda_o$ at a temperature shift $\delta T/2$, the output power is changed to the half of resonant dip. Therefore, the temperature shift δT behaves as the FWHM of the resonance in the temperature tuning domain. The relationship between δT and $\delta\lambda_o$ can be obtained directly by considering the resonant condition of the resonator at m-order resonance of λ_m at temperature T with waveguide mode group index $n_g = n_{eff} - \partial n_{eff}/\partial\lambda_o$, the resonant wavelength changes with temperature:

$$\frac{d\lambda_m}{dT} = \frac{\lambda_m}{n_g}\frac{\partial n_{eff}}{\partial T}\bigg|_{\lambda_m}, \quad \text{then} \quad \delta\lambda_o \cong \frac{\lambda_m}{n_g}\frac{\partial n_{eff}}{\partial T}\bigg|_{\lambda_m}\delta T. \tag{3}$$

The thermo-optic coefficient of the waveguide mode can be obtained by considering temperature difference between two resonances in temperature domain, ΔT, of same wavelength λ_o:

$$\frac{\partial n_{eff}}{\partial T}\bigg|_{\lambda_o} \cong \frac{\lambda_o}{L_{rt}\Delta T}. \tag{4}$$

By combining (3) and (4), Q can be expressed as

$$Q = \frac{\lambda_m}{\delta\lambda_o} \cong \frac{\Delta T}{\delta T}\frac{n_g L_{rt}}{\lambda_m}. \tag{5}$$

From the thermal transmission curves at 1546 nm, shown in Fig. 4(c) and (d), the resonant period ΔT is and FWHM δT are 24.7 $\pm$ 1.0 °C and 0.74 $\pm$ 0.03 °C, respectively. The mode group index is 4.35 which is obtained by $FSR = \lambda_m^2/n_g L_{rt}$. By (5), the resulting Q is about 24800 $\pm$ 2000. The measured values of Q from the wavelength scanning and thermal tuning techniques agree to within the error bars of the different measurement techniques.

By combining (5) and $FSR = \lambda_m^2/n_g L_{rt}$

$$\frac{\Delta T}{\delta T} \cong \frac{FSR}{\delta\lambda_o} = F. \tag{6}$$

This gives similar results as obtained by assuming $\Delta T/\delta T$ as being equal to the finesse [21].

As this proposed method works well in near-IR, it was applied in the SOS microring resonators at mid-IR. From Fig. 3(b), the resonant period ΔT and dip FWHM δT are 11.2 $\pm$ 0.4 °C and 1.48 $\pm$ 0.06 °C, respectively. The theoretical mode effective index is 4.01 calculated by FEM. The resulting Q is about 11400 $\pm$ 800. Since the power stability and the linewidth of the ZBLAN fiber laser is not as good as the commercial tunable laser, the measurement results of our system, in fact, are the convolution of the actual resonator transmission spectral function and the power spectrum of the laser. Therefore, the features would be averaged or broadened. The estimated Q factor may be underestimated. Using this method with a narrow linewidth laser (such as a mid-IR He-Ne laser), the maximum measurable Q can be up to 10^6 by using a temperature controller system with temperature stability and set point resolution in 0.01 °C, which is commercially available. This limit is over 10 times of wavelength scanning with QCLs.

4.3. Thermo-optic Coefficient

The thermo-optic coefficient of the waveguide mode, from (4), can be used to estimate the thermo-optic coefficient of the epitaxial silicon core, $\partial n_{Si}/\partial T$, of SOS by the perturbation method [22], [23]. This method is more accurate than conventional mode weighted average method for high

index contrast waveguide [28]. A small perturbation of the waveguide materials refractive indices induces the small change of effective index in waveguide mode δn_{eff}:

$$\delta n_{eff} \cong \frac{\int_{\infty} \left(\frac{\partial n(r)}{\partial T}\delta T\right) n(r)|E|^2 dr}{Z_o \int_{\infty} \mathrm{Re}\{E \times H^*\} \cdot e_z dr} \cong \Gamma_{Si} \frac{n_g}{n_{Si}} \frac{\partial n_{Si}}{\partial T} \delta T, \text{ with } \Gamma_{Si} = \frac{\int_{Si} n(r)^2 |E|^2 dr}{\int_{\infty} n(r)^2 |E|^2 dr} \tag{7}$$

$$\frac{\partial n_{eff}}{\partial T} \cong \frac{\delta n_{eff}}{\delta T} \cong \Gamma_{Si} \frac{n_g}{n_{Si}} \frac{\partial n_{Si}}{\partial T} \tag{8}$$

where Z_o is the impedance of vacuum, and Γ_{Si} is defined as the conventional electric field confinement factor of the mode in silicon core region. In (7), because of the thermo-optic coefficients of sapphire and air is much smaller than silicon [29], [30], and the electric field is highly confined in the silicon core, we can neglect the contribution of them. Moreover, the high thermal conductivity of silicon ensures the temperature can be approximately constant in the core. Again, we start from the SOI counterpart in near-IR. The $\partial n_{eff}/\partial T$ is obtained as $2.37 \pm 0.10 \times 10^{-4}$ K^{-1} and then the resulting $\partial n_{Si}/\partial T$ of silicon core of SOI is $2.07 \pm 0.08 \times 10^{-4}$ K^{-1} which agrees well to the result in [16]. The value is smaller than the waveguide mode thermo-optic coefficient since $\Gamma_{Si} \cdot n_g/n_{Si}$ is larger than 1. It is because n_g is larger than n_{Si} while Γ_{Si} is close 1. It indicates that the light in guided mode with large group index spends more time, therefore, experience higher thermo-optic effect than in bulk material for given a length [23].

In case of SOS microring, $\partial n_{eff}/\partial T$ and theoretical group index are obtained as $2.38 \pm 0.08 \times 10^{-4}$ K^{-1} and 4.01, respectively. Then $\partial n_{Si}/\partial T$ of epitaxial silicon on SOS is $2.11 \pm 0.08 \times 10^{-4}$ K^{-1}. We can see that the resulting value of epitaxial silicon on SOS is similar to the bulk silicon.

5. Conclusion

In conclusion, we have fabricated and characterized microring resonators on SOS at wavelength of 2.75 μm by thermal tuning. The measured Q factor was about 11400 ± 800 under normal ($\sim$60% relative humidity) atmospheric condition. The thermo-optic coefficient of epitaxial silicon on SOS is estimated as $2.11 \pm 0.08 \times 10^{-4}$ K^{-1} by perturbation method. The characterization methods have been verified by SOI microring in near-IR with comparable results. The thermal tuning technique for Q factor measurement is of practical use for characterizing resonator at wavelengths where there is limited tunability and spectral resolution of laser source and the technique may find applications for other types of cavities such as Fabry–Pérot cavities in mid-IR.

Acknowledgment

We thank Bookham (now Oclaro Inc) for the 975 nm pump laser.

References

[1] R. A. Soref, S. J. Emelett, and W. R. Buchwald, "Silicon waveguided components for the long-wave infrared region," *J. Opt. A, Pure Appl. Opt.*, vol. 8, no. 10, pp. 840–848, Oct. 2006.
[2] G. T. Reed, *Silicon Photonics: The State of the Art*. Hoboken, NJ: Wiley, 2008.
[3] T. K. Liang and H. K. Tsang, "Role of free carriers from two-photon absorption in Raman amplification in silicon-on-insulator waveguides," *Appl. Phys. Lett.*, vol. 84, no. 15, pp. 2745–2747, Apr. 2004.
[4] V. Raghunathan, D. Borlaug, R. R. Rice, and B. Jalali, "Demonstration of a Mid-infrared silicon Raman amplifier," *Opt. Exp.*, vol. 15, no. 22, pp. 14 355–14 362, Oct. 2007.
[5] B. Jalali, V. Raghunathan, R. Shori, S. Fathpour, D. Dimitropoulos, and O. Stafsudd, "Prospects for silicon mid-IR raman lasers," *IEEE J. Sel. Topics Quantum Electron.*, vol. 12, no. 6, pp. 1618–1627, Nov./Dec. 2006.
[6] X. Liu, R. M. Osgood, Y. A. Vlasov, and W. M. J. Green, "Mid-infrared optical parametric amplifier using silicon nanophotonic waveguides," *Nat. Photon.*, vol. 4, no. 8, pp. 557–560, Aug. 2010.
[7] B. Kuyken, X. Liu, G. Roelkens, R. Baets, R. M. Osgood, and W. M. J. Green, "50 dB parametric on-chip gain in silicon photonic wires," *Opt. Lett.*, vol. 36, no. 22, pp. 4401–4403, Nov. 2011.
[8] R. Shankar, R. Leijssen, I. Bulu, and M. Lonèar, "Mid-infrared photonic crystal cavities in silicon," *Opt. Exp.*, vol. 19, no. 6, pp. 5579–5586, Mar. 2011.

[9] G. Z. Mashanovich, M. M. Milošević, M. Nedeljkovic, N. Owens, B. Xiong, E. J. Teo, and Y. Hu, "Low loss silicon waveguides for the mid-infrared," *Opt. Exp.*, vol. 19, no. 8, pp. 7112–7119, Apr. 2011.
[10] T. Baehr-Jones, A. Spott, R. Ilic, A. Spott, B. Penkov, W. Asher, and M. Hochberg, "Silicon-on-sapphire integrated waveguides for the mid-infrared," *Opt. Exp.*, vol. 18, no. 12, pp. 12 127–12 135, Jun. 2010.
[11] F. Li, S. D. Jackson, C. Grillet, E. Magi, D. Hudson, S. J. Madden, Y. Moghe, C. O'Brien, A. Read, S. G. Duvall, P. Atanackovic, B. J. Eggleton, and D. J. Moss, "Low propagation loss silicon-on-sapphire waveguides for the mid-infrared," *Opt. Exp.*, vol. 19, no. 16, pp. 15 212–15 220, Aug. 2011.
[12] A. Spott, Y. Liu, T. Baehr-Jones, R. Ilic, and M. Hochberg, "Silicon waveguides and ring resonators at 5.5 μm," *Appl. Phys. Lett.*, vol. 97, no. 21, p. 213 501, 2010.
[13] N. Carlie, J. D. Musgraves, B. Zdyrko, I. Luzinov, J. Hu, V. Singh, A. Agarwal, L. C. Kimerling, A. Canciamilla, F. Morichetti, A. Melloni, and K. Richardson, "Integrated chalcogenide waveguide resonators for mid-IR sensing: Leveraging material properties to meet fabrication challenges," *Opt. Exp.*, vol. 18, no. 25, pp. 26 728–26 743, Dec. 2010.
[14] G. J. Veldhuis, O. Parriaux, H. J. W. M. Hoekstra, and P. V. Lambeck, "Sensitivity enhancement in evanescent optical waveguide sensors," *J. Lightwave Technol.*, vol. 18, no. 5, pp. 677–682, May 2000.
[15] A. Densmore, D.-X. Xu, P. Waldron, S. Janz, P. Cheben, J. Lapointe, A. Delage, B. Lamontagne, J. H. Schmid, and E. Post, "A silicon-on-insulator photonic wire based evanescent field sensor," *IEEE Photon. Technol. Lett.*, vol. 18, no. 23, pp. 2520–2522, Dec. 2006.
[16] G. Cocorullo and I. Rendina, "Thermo-optical modulation at 1.5 μm in silicon etalon," *Electron. Lett.*, vol. 28, no. 1, pp. 83–85, Jan. 1992.
[17] D.-X. Xu, M. Vachon, A. Densmore, R. Ma, S. Janz, A. Delage, J. Lapointe, P. Cheben, J. H. Schmid, E. Post, S. Messaoudene, and J.-M. Fedeli, "Real-time cancellation of temperature induced resonance shifts in SOI wire waveguide ring resonator label-free biosensor arrays," *Opt. Exp.*, vol. 18, no. 22, pp. 22 867–22 879, Oct. 2010.
[18] B. J. Frey, D. B. Leviton, and T. J. Madison, "Temperature-dependent refractive index of silicon and germanium," in *Proc. SPIE*, Orlando, FL, 2006, vol. 6273, p. 627 32J.
[19] X. S. Zhu and R. Jain, "Numerical analysis and experimental results of high-power Er/Pr:ZBLAN 2.7 μm fiber lasers with different pumping designs," *Appl. Opt.*, vol. 45, no. 27, pp. 7118–7125, Sep. 2006.
[20] C. Y. Wong, Z. Cheng, X. Chen, K. Xu, C. K. Y. Fung, Y. Chen, and H. K. Tsang, "Mid-infrared micro-ring resonator on silicon-on-sapphire characterized by thermal tuning," in *Proc. IEEE IPC*, Arlington, VA, 2011, pp. 877–878.
[21] R. Adar, Y. Shani, C. H. Henry, R. C. Kistler, G. E. Blonder, and N. A. Olsson, "Measurement of very low-loss silica on silicon waveguides with a ring resonator," *Appl. Phys. Lett.*, vol. 58, no. 5, pp. 444–445, Feb. 1991.
[22] T. Baehr-Jones, M. Hochberg, C. Walker, E. Chan, D. Koshinz, W. Krug, and A. Scherer, "Analysis of the tuning sensitivity of silicon-on-insulator optical ring resonators," *J. Lightwave Technol.*, vol. 23, no. 12, pp. 4215–4221, Dec. 2005.
[23] J. T. Robinson, K. Preston, O. Painter, and M. Lipson, "First-principle derivation of gain in high-index-contrast waveguides," *Opt. Exp.*, vol. 16, no. 21, pp. 16 659–16 669, Oct. 2008.
[24] M. Bass, C. DeCusatis, J. Enoch, V. Lakshminarayanan, G. Li, C. MacDonald, V. Mahajan, and E. Van Stryland, *Handbook of Optics,* 3rd ed. New York: McGraw-Hill, 2009.
[25] Z. Cheng, X. Chen, C. Y. Wong, K. Xu, C. K. Y. Fung, Y. M. Chen, and H. K. Tsang, "Mid-infrared grating couplers for silicon-on-sapphire waveguides," *IEEE Photon. J.*, vol. 4, no. 1, pp. 104–113, Feb. 2012.
[26] A. Yariv, "Universal relations for coupling of optical power between microresonators and dielectric waveguides," *Electron. Lett.*, vol. 36, no. 4, pp. 321–322, 2000.
[27] Y. Okada and Y. Tokumaru, "Precise determination of lattice parameter and thermal expansion coefficient of silicon between 300 and 1500 K," *J. Appl. Phys.*, vol. 56, no. 2, pp. 314–320, Jul. 1984.
[28] T. J. Johnson, M. Borselli, and O. Painter, "Self-induced optical modulation of the transmission through a high-*Q* silicon microdisk resonator," *Opt. Exp.*, vol. 14, no. 2, pp. 817–831, Jan. 2006.
[29] D. Yang, M. E. Thomas, and S. G. Kaplan, "Measurement of the infrared refractive index of sapphire as a function of temperature," in *Proc. SPIE*, Orlando, FL, 2001, vol. 4375, pp. 53–63.
[30] M. Pokrass, Z. Burshtein, and R. Gvishi, "Thermo-optic coefficient in some hybrid organic/inorganic fast sol–gel glasses," *Opt. Mater.*, vol. 32, no. 9, pp. 975–981, Jul. 2010.